ISBN: 978-3-95450-220-2 ISSN: 2673-5474 doi: 10.18429/JACoW-FEL2022-WEP20

ACHIEVEMENTS AND CHALLENGES FOR SUB-10 fs LONG-TERM ARRIVAL TIME STABILITY AT LARGE-SCALE SASE FEL FACILITIES

B. Lautenschlager*, M. K. Czwalinna, J. Kral, J. Müller, S. Pfeiffer,
H. Schlarb, C. Schmidt, S. Schulz, M. Schütte, B. Steffen
Deutsches Elektronen-Synchrotron DESY, Notkestr. 85, 22607 Hamburg, Germany

Abstract

A high temporal stability of produced photon pulses is a key parameter for some classes of experiments, e.g., those using a pump-probe scheme. A longitudinal intra bunch-train feedback system, that reduces the intra bunch-train and the train-to-train arrival time fluctuations down to the sub-10 fs level was implemented at the European X-ray free electron laser (EuXFEL). The low arrival time jitter of the electron beam is preserved in the generated photon pulses. However, over long measurement periods, additional environmental factors acting on different time scales have to be considered. These factors include the temperature, relative humidity and in case of the European XFEL ground motions due to ocean activities. Mitigation of the residual timing drifts between pump laser and FEL pulses requires additional measures to disentangle the overlaid effects. The latest results and future challenges for the long-term arrival time stabilization will be presented.

INTRODUCTION

The European XFEL (EuXFEL) is a free electron laser facility with a 2 km long superconducting electron accelerator and a total length of 3.4 km. The facility operates in a 10 Hz burst mode with an RF pulse length of 600 µs. Each RF pulse can accelerate up to 2700 bunches with the maximum repetition rate of 4.5 MHz. The superconducting radio frequency (SRF) cavities accelerate the electron bunch-trains up to an electron beam energy of 17.5 GeV. Three undulator beamlines can be used to provide photon pulses to the different experiments.

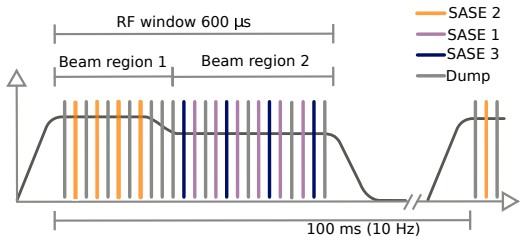

Figure 1: Schematic of the electron bunch distribution to the different SASE beamlines and the dump [1].

A system of slow and fast kickers distributes the electron bunches into the three different undulator beamlines and a dump, see Fig. 1. Photon energies in the range from 0.25 to 25 keV can be provided, using different linac energies and variable gap undulators. A three stage compression scheme, with the three magnetic chicanes, BC1, BC2, and BC3 can be used to influence the longitudinal parameters, like the compression and arrival time. The RF pulse can be separated into different beam regions, with different RF parameters in amplitude and phase, in order to provide individual compression schemes for the beamlines [2].

A longitudinal intra bunch-train feedback (L-IBFB) adjusts the electron bunch energies in front of a magnetic bunch compression chicane by actuating the preceding accelerator's module amplitude and phase. This introduces an energy dependent path length of the electron bunches through the chicane and thus a change of the arrival time. The bunch arrival time monitors (BAMs) measure the relative arrival time of the electron bunches, with a resolution down to 3 fs [1], against a femtosecond stable optical reference system [3]. The laser based synchronization system is also used to synchronize the lasers in the experimental hutches. An overview of optical reference system can be found in [4].

The low-level radio frequency (LLRF) system controls the 1.3 GHz RF field of the SRF cavities in phase and amplitude. An optical reference module (REFM-OPT) is used to resynchronize the RF phase with respect to the laser pulses, coming from the optical synchronization system, to compensate for drifts in the 1.3 GHz RF reference distribution chain, due to humidity and temperature variations [5]. Different controllers are combined in the LLRF system to achieve the typical RF field stability in amplitude of $\Delta A/A \approx 0.008$ % and in phase of $\Delta\Phi \approx 0.007$ deg [6, 7]. A second order multiple-input multiple-output controller is used to react within a bunch-train. To minimize repetitive errors from bunch-train to bunch-train a learning feedforward control algorithm is applied. A combination of the measured field information in amplitude and phase and beam-based measurements, e.g., the arrival time, is included in the LLRF control strategy and introduced in [8, 9]. This combination is used by the L-IBFB to stabilize the the electron bunch arrival time below 10 fs (rms) [1].

ARRIVAL TIME MEASUREMENT AND STABILIZATION AT THE EUROPEAN XFEL

A schematic of the EuXFEL facility is shown in Fig. 2. The bunch arrival time monitors provide the arrival time bunch-by-bunch using an electro-optical detection scheme. The electromagnetic field of the electron bunches is captured by four broadband (40 GHz) RF pickups. The induced RF signal is sampled by an ≈ 200 fs laser pulse of the optical ref-

* bjoern.lautenschlager@desy.de

ISBN: 978-3-95450-220-2 ISSN: 2673-5474 doi: 10.18429/JACoW-FEL2022-WEP20

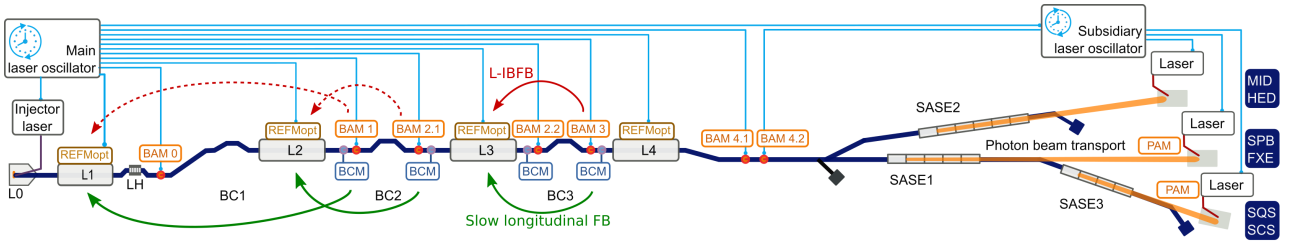

Figure 2: Schematic of the EuXFEL facility with the diagnostic units, like the bunch arrival time monitor (BAM) and bunch compression monitor (BCM), the distribution of the optical reference system (blue lines), the feedback loops (red and green lines) and the the different accelerator parts L1, L2, L3 and L4, which are including the SRF modules and the LLRF system [1].

erence system, within a Mach-Zehnder type electro-optical modulator. The passing light amplitude is modulated by the RF field, such that the strength of the modulation is proportional to the arrival time variations of the single electron bunches [10–12]. Further developments and optimizations of the past years of the BAMs and the optical synchronization system has led to relative electron bunch arrival time measurements with a resolution down to 3 fs [1].

The arrival time of the generated FEL pulses is measured by photon arrival time monitors (PAMs), which are however exclusive to some user experiments. A detailed description can be found in [13]. It has been verified by correlations between BAM and PAM measurements, that the electron bunch arrival time jitter is preserved for the FEL pulses during the SASE process [1].

The BAM measurements are used in feedback loops to reduce the arrival time jitter to the sub-10 fs level. At locations in the accelerator with a significant longitudinal dispersion, any change in beam energy gain upstream of such a dispersive section results in an arrival time change downstream of it. This effect is exploited in the combination of two longitudinal feedbacks, an intra-train loop for correcting fast fluctuations, and a slow loop for compensation of drifts to keep to L-IBFB in its dynamic operation range. At EuXFEL, those feedback combinations are implemented for the RF stations directly upstream of the three bunch compression chicanes, BC1, BC2 and BC3.

The LLRF controller uses a combined and weighted error signal of the RF field measurements together with the beam-based measurements, e.g. the arrival time, to control the amplitude and phase of the RF station and thus the energy prior to a chicane in order to stabilize the arrival time [9]. The longitudinal feedback for slow drift compensation uses the compression and energy or arrival time as monitor signal and the sum-voltage and chirp of one accelerator section as actuator. For timing critical experiments at the EuXFEL the combination of the L-IBFB at L3 (red solid line, Fig. 2) and the slow feedbacks at all locations (green solid lines, Fig. 2) are permanently activated and used in standard operation.

After BC3, the accelerator part L4 increases the beam energy without influencing the arrival time, such that the two monitors, BAM4.1 and BAM 4.2, located 1.5 km apart from BAM3 can be used as out-of-loop monitors. The two monitors BAM3 and BAM4.1 show an excellent correlation (0.99 Pearson's coefficient over 1 minute of data) for the bunch-train mean values with a correlation width of 1.15 fs [1].

RESULTS

This section presents the results of the short term arrival time measurements with activated L-IBFB , as well as, long term comparison between the BAM3 and BAM4.1 over days. The presented data were acquired with an electron bunch repetition of 2.25 MHz and a typical charge of 250 pC. Each bunch train included over 800 bunches. Figure 3 shows the

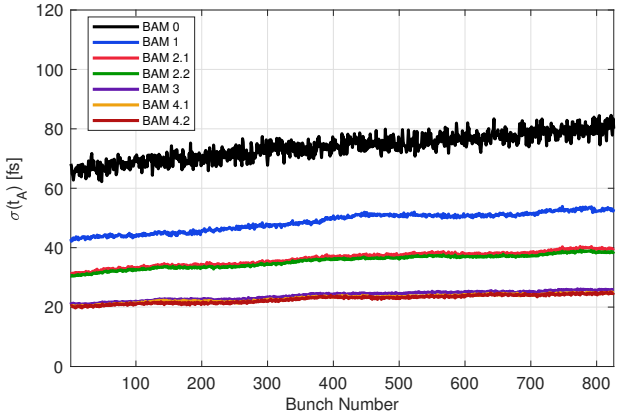

Figure 3: Arrival time jitter $\sigma(t_A)$ with the L-IBFB disabled at different BAM locations, starting with the BAM0 in the injector section and ends with the BAM4.2 at the end of the acceleration part. Each line represents the standard deviation of 600 consecutive bunch-trains with a bunch-to-bunch repetition rate of 2.25 MHz.

evolution of the measured arrival time jitter $\sigma(t_A)$ along the accelerator, starting with an incoming arrival time jitter of $\approx$ 70 fs (rms, mean of the bunch-train) measured with the BAM0 (black solid line) in the injector section. The jitter is reduced with each compression stage to the final value of $\approx$22 fs (rms, mean of the bunch-train) measured consistently with the three equivalent monitors BAM3, BAM4.1 and BAM4.2. The arrival time jitter (standard deviation) is

ISBN: 978-3-95450-220-2 ISSN: 2673-5474 doi: 10.18429/JACoW-FEL2022-WEP20

calculated from 600 consecutive bunch-trains, which corresponds to one minute of data.

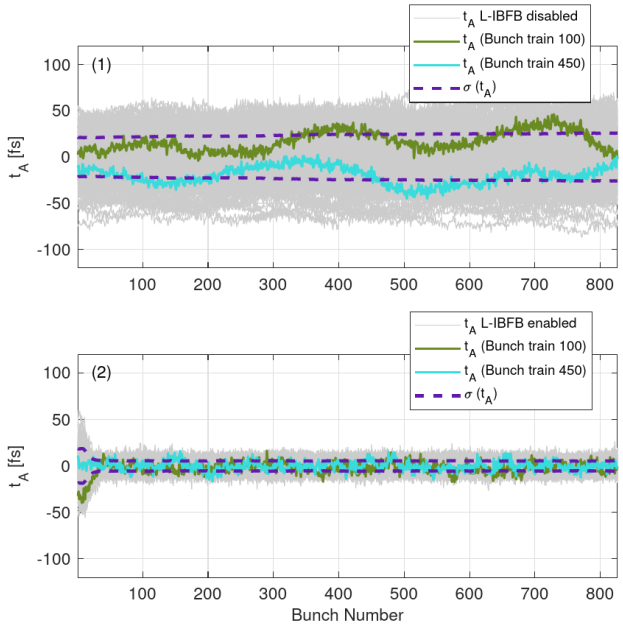

Figure 4: Comparison of the arrival time data of 600 bunch-trains, where the mean arrival time had been subtracted from each bunch train, with the L-IBFB disabled (first plot) and with the L-IBFB activated (second plot). The gray lines are the arrival time of the individual bunch-trains with two highlighted bunch-trains (100 and 450, colored lines) and the purple dashed lines are the standard deviation of the 600 bunch-trains and represents the arrival time jitter $\sigma(t_A)$.

Figure 4 shows the mean free arrival time measured with the BAM3 after the third chicane BC3. The first plot shows the situation with the L-IBFB disabled, and in comparison to that, the second plot shows the measured arrival time and standard deviation with the L-IBFB activated at L3. The comparison of the two plots shows how the L-IBFB acts from bunch-to-bunch at the beginning of the bunch-train. The peak-to-peak value is reduced significantly within the first few bunches until the final stabilized arrival time is reached. Figure 5 shows the same effect by comparing the arrival time jitter directly. The black line represents the arrival time jitter with the L-IBFB disabled and a mean jitter value of above 20 fs (rms). That value is pushed down by the longitudinal intra bunch-train feedback below 6 fs (rms, purple line), which corresponds to a tremendous improvement of the arrival time stability by a factor of 4. The steady state arrival time jitter is reached after an adaption time of ≈15 µs (30–40 bunches with a repetition rate of 2.25 MHz). The kicker distribution system diverts the first few bunches from the transient region into the dump, such that only the highly stabilized bunches are used for the SASE process (compare Fig. 1).

The L-IBFB operates together with the slow longitudinal feedback over days in order to achieve a highly stabilized arrival time, which is shown in the first plot of Fig. 6.

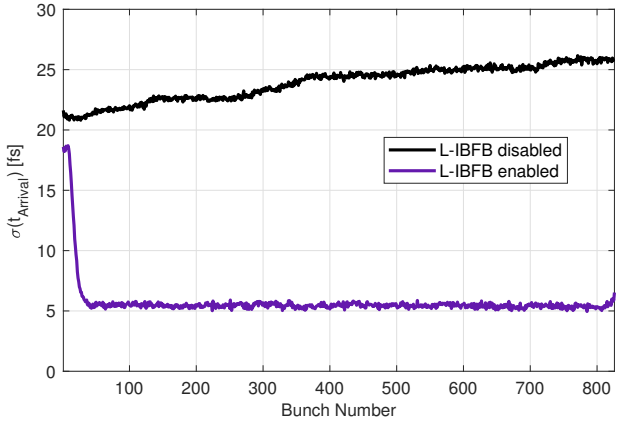

Figure 5: Comparison of the arrival time jitter, with the L-IBFB disabled and enabled, measured with the in-loop BAM3 after the third chicane BC3. The standard deviation is computed over the same 600 consecutive bunch-trains as before.

The comparison to the measurement with the out-of-loop BAM4.1 (second plot, Fig. 6), in 1.5 km distance, shows a long range baseline fluctuation over days. Although, there is no section with a significant longitudinal dispersion in between the BAM3 and BAM4.1. The out-of-loop arrival time measurement shows a clear oscillation with a period of ≈ 12 h and a variation of roughly ±150 fs.

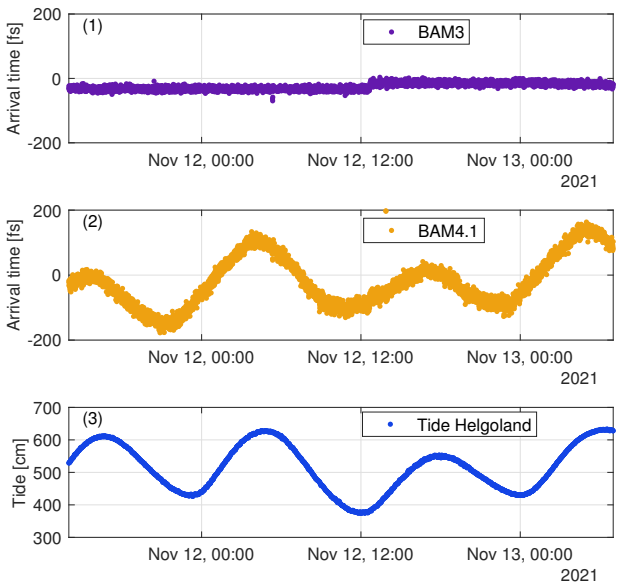

Figure 6: Comparison of long term arrival time measurements. The first plot shows the arrival time measured with the in-loop BAM3. The second plot shows the arrival time measured with the out-of-loop BAM4.1. The third plot shows the tide at the North Sea, *Source of the tidal data: www.pegelonline.wsv.de*.

The proximity to the North Sea, the 12 h period and the comparison to the measured tide, shown in the third plot of Fig. 6, suggests that these arrival time drifts could be

ISBN: 978-3-95450-220-2 ISSN: 2673-5474 doi: 10.18429/JACoW-FEL2022-WEP20

correlated to physical length changes of the accelerator, due to ground motions induced by the tidal range. The observed timing drifts are manifest, as well as, fluctuations between the photon pulses arrival time and the stabilized optical synchronization timing that drives the user experiment.

CONCLUSION

The presented results show that the arrival time stability is improved significantly, by a factor of 4, down to the 6 fs (rms) level, when using the longitudinal intra bunch-train feedback. Long term fluctuations, with a period of ≈12 h were observed in between two distant arrival time measurement stations 1.5 km apart from each other. These fluctuations closely resemble the local tide in the main parameters, like the 12 h period. The induced timing variation in the order of hundreds of femtoseconds is detrimental to long-term averaging timing sensitive experiments. Investigations of the exact magnitude and its mitigation is ongoing.

OUTLOOK

To investigate and compensate for the long term arrival time instabilities several upgrades and developments are ongoing. A new laser pulse arrival time monitor (LAM) is under development. The LAM could be used to measure the arrival time of the probe laser pulses in the experimental hutches, to detect and compensate for arrival time drifts, due to temperature or humidity changes. The last arrival time measurement is 1.5 km apart from the experimental hutches and the propagation of the arrival time drifts are unknown at the moment. Three new BAMs will be installed directly after each undulator section. These SASE BAMs will be used to investigate and evaluate the arrival time drifts further and could be used to compensate for the observed arrival time drifts. Other effects recently observed in the arrival time difference between two BAMs 1.5 km apart from each other, with a frequency of 0.2 Hz are under investigation and could be linked to ground motions induced by ocean waves.

REFERENCES

[1] M. K. Czwalinna *et al.*, "Beam Arrival Stability at the European XFEL", *Proc. IPAC2021*, Campinas, SP, Brazil, 2021. doi:10.18429/JACoW-IPAC2021-THXB02

[2] W. Decking *et al.*, "A MHz-repetition-rate hard X-ray free-electron laser driven by a superconducting linear accelerator", *Nat. Photonics*, vol. 14, pp. 391-397, 2020. doi:10.1038/s41566-020-0607-z

[3] F. Löhl *et al.*, "Electron Bunch Timing with Femtosecond Precision in a Superconducting Free-Electron Laser", *Physical Review Letters*, vol. 104, no. 14, p. 144 801, 2010. doi:10.1103/PhysRevLett.104.144801

[4] S. Schulz *et al.*, "Femtosecond all-optical synchronization of an x-ray free-electron laser", *Nature Communications*, vol. 6, pp. 5938–5949, 2015. doi:10.1038/ncomms6938

[5] T. Lamp *et al.*, "Femtosecond Laser-to-RF Synchronization and RF Reference Distribution at the European XFEL", in *Proc. FEL2019*, Hamburg, Germany, 2019, pp. 343-345. doi:10.18429/JACoW-FEL2019-WEP010.

[6] C. Schmidt *et al.*, "Recent Developments of the European XFEL LLRF System", in *Proc. IPAC'13*, Shanghai, China, 2013, paper WEPME009, pp. 2941–2943.

[7] M. Omet *et al.*, "LLRF Operation and Performance at the European XFEL", in *Proc. IPAC2018*, Vancouver, BC, Canada, 2018, pp. 1934–1936. doi:10.18429/JACoW-IPAC2018-WEPAF051.

[8] S. Pfeiffer,"Symmetric grey box identification and distributed beam-based controller design for free-electron lasers", Ph.D. thesis, TUHH, Hamburg, Germany, 2014.

[9] S. Pfeiffer *et al.*, "Fast Feedback Strategies for Longitudinal Beam Stabilization", in *Proc. IPAC'12*, 2012, paper MOOAA03, pp. 26–28.

[10] M. Viti *et al.*,"The Bunch Arrival Time Monitor at FLASH and European XFEL", in *Proc. ICALEPCS'17*, Barcelona, Spain, 2017, pp. 701–705. doi:10.18429/JACoW-ICALEPCS2017-TUPHA125

[11] A. Angelovski *et al.*, "Evaluation of the cone-shaped pickup performance for low charge sub-10 fs arrival-time measurements at free electron laser facilities", *Phys. Rev. ST Accel. Beams*, vol. 18, no. 1, p. 012 801, 2015. doi:10.1103/PhysRevSTAB.18.012801

[12] M. K. Czwalinna *et al.*, "New design of the 40 GHz bunch arrival time monitor using MTCA.4 electronics at FLASH and for the European XFEL", in *Proc. IBIC'13*, Oxford, United Kingdom, 2013, paper WEPC31, pp. 749–752.

[13] H. J. Kirkwood *et al.*, "Initial observations of the femtosecond timing jitter at the European XFEL", in *Optics Letters*, vol. 44, pp. 1650-1653, 2019. doi:10.1364/OL.44.001650